INTERNATIONAL JOURNAL OFAUTOMOTIVE AND MECHANICAL ENGINEERING (IJAME)
ISSN: 2229-8649 e-ISSN: 2180-1606
VOL.XX, ISSUEXX,XXX –XXX
DOI: https://doi.org/10.15282/ijame.v#i#.###

ORIGINAL ARTICLE

Optimization Design of Electromechanical Servo System based on Dual Motor Control Algorithm

Wei Lu

School of Mechanical Engineering, Wuxi Institute of Technology, 214121 Wuxi, China

ABSTRACT –The control accuracy and performance of current servo systems are greatly challenged. For this reason, how to effectively improve the control effect of the servo system and encoder accuracy, has become the focus of current research. Therefore, the research aims to improve the control effect and encoder accuracy of electromechanical servo systems. Moreover, the dual-motor control algorithm is innovatively used to optimize and analyze the electromechanical servo system. The study achieves more accurate load control by coordinating the synchronized operation of the two motors, which in turn improves the overall performance of the motor servo system. The dual-motor control algorithm achieves more precise control of the load by coordinating the synchronized operation of the two motors, thus enhancing the overall performance of the motor servo system. The results show that after the algorithm optimization, the maximum rotational angular velocity of the system reaches 160 rpm, and the angular velocity changes significantly in the time range of 0-50 ms. This shows that the use of a dual-motor control algorithm can effectively improve the motor control capability. This is an important guiding significance for the research of motor servo system.

ARTICLE HISTORY
Received:xxxx
Revised:xxxx
Accepted:xxxx
Published: xxxx

KEYWORDS
Electromechanical
Servo system
DMCA
Accuracy
Control

Pre-Proof Copy

1.0 INTRODUCTION

In modern industrial and military fields, electromechanical servo systems, as a key automatic control device, are widely used in high-precision and cutting-edge equipment such as radar, aerospace, and CNC machine tools [1]. The performance of the servo system directly affects the response speed, positioning accuracy, and overall efficiency of the equipment [2]. Therefore, how to effectively improve the control effect of electromechanical servo systems and enhance their dynamic response and steady-state performance has become an important research topic. In recent years, with the rapid development of control theory and computing technology, the Dual Motor Control Algorithm (DMCA) has gradually gained widespread attention due to its advantages in improving system redundancy, increasing output power, and improving control accuracy [3]. DMCA can achieve more precise control of the load and higher dynamic performance by coordinating the synchronous operation of two motors, thereby significantly improving the overall performance of the electromechanical servo system [4].

To address the issue of poor accuracy in electromechanical servo systems, Thangavel et al. [5] designed a servo electromechanical system and established a new mathematical model for the system using the DMCA. The research results indicated that the system had the advantages of compact structure, easy control, high precision, reliability, linearity, and high aspect ratio. Aimasso et al. [6] proposed a new simplified monitoring model to solve the problem of the lack of predictive function in flight command electromechanical servo systems, which accurately reproduced the dynamic response of typical aerospace electromagnetic radiation. The system evaluation results indicated that the new model was experimentally validated in MATLAB-Simulink and could predict the impending failure of the flight command electromechanical brake. He et al. [7] proposed a composite control method based on DMCA for sliding mode and self-disturbance rejection control to address the difficulty of cutting head control in electromechanical servo systems under parameter changes and disturbance uncertainties. On the basis of traditional active disturbance rejection control, the fastest discrete tracking differentiator and extended state observer were designed. The research results indicated that the new control method improved the tracking accuracy and robustness of the position servo system. Chen et al. [8] proposed a robust indirect adaptive controller based on a nonlinear x-exchange technique for high-precision motion control of electromechanical servo systems with time-varying parameter estimation. The adaptive feed-forward cancellation technique could effectively compensate for the uncertainty of time-varying parameters. The experimental results verified that the estimation results obtained by the proposed control strategy had good asymptotic tracking performance.

Hu et al. [9] proposed a practical adaptive robust control method based on a dual valve parallel electromechanical servo system to meet the requirements of modern mobile machinery for trajectory tracking accuracy and high efficiency. This method eliminated parameter uncertainty and load disturbances, incorporated the DMCA, and solved the problem of flow redundancy. The research results verified the effectiveness of the new method, which could effectively achieve tracking accuracy and flow distribution through simple on-site parameter adjustment. In their study, Hossain MS et al.

*CORRESPONDING AUTHOR |W. Lu | ✉tianbao9501@163.com

© The Authors2019. Published by Penerbit UMP. This is an open access article under the CC BY license.

used variable timing and fast-operating control valves for the control of electromechanical follower systems, which are capable of providing precise and adaptive control mechanisms at the inlet of the expander. Through valve optimization and control, the system performance of a gas expander could be significantly improved. The methodology used in the current study was theoretically capable of improving the cycle performance parameters through a multistage unstructured fuzzy decision analysis approach. However, the method lacked practical application results, while the high cost of use limited the popularity of the research method [10]. In the study by Zhang L et al., research was carried out to establish a 3D simulation model by integrating a fuzzy Proportional-Integral-Derivative (PID) control algorithm. The new model could help the electromechanical follower system for testing and optimization. The results of the study showed that the new electromechanical control follower system had a significant improvement in control and management efficiency by about 30% compared to the conventional system. The current method is able to improve the efficiency of the follower system and reduce operating costs. However, the increased difficulty of the operation of the method makes it difficult to popularize and promote it, making the new method more limited [11]. A linear Electromechanical Actuator (EMA) was used to control the electromechanical follower system in the study of Hashim AA et al. Meanwhile, the new method introduced meta-heuristics, Spiral Dynamic Algorithms (SDAs), and an artificial swarming algorithm to optimize the PI parameters and thus control the position of the EMA. The results showed that the PI controller optimized by the SDA and Artificial Bee Colony (ABC) algorithms exhibited excellent performance, which is able to effectively reduce the steady state error and overshoot of the system and improve the system's rise time and stable response time. Although the new method could improve the system control accuracy and enhance the fast response of the system, the new method had higher resources for computation, and the computing cost was also increased accordingly [12]. It can be seen that although the latest research methods can effectively improve the operational performance of the system, their usability and cost need to be further improved.

In summary, most of the previous research on electromechanical servo systems is mainly aimed at reducing dynamic noise and composite control issues of the system. However, in most current research, there are still problems, such as poor control accuracy and poor system control effectiveness in electromechanical servo systems. Based on this, to improve the control accuracy and effectiveness of the system, the DMCA is studied to optimize and improve the design of the electromechanical servo system. This study aims to control the electromechanical servo system by constructing a torque system and innovatively incorporates a dual electromechanical control algorithm to improve the control accuracy of the electromechanical servo system. Moreover, the PID control system is used to optimize the algorithmic program. At the same time, it can improve and optimize the encoder of the electromechanical servo system to enhance the control effect optimization of the system. Table 1 shows all abbreviations that appear throughout the entire text.

Table 1 List of Abbreviations

Abbreviation	Full name
DMCA	Dual Motor Control Algorithm
PID	Proportional-Integral-Derivative Control
SPI	Serial Peripheral Interface
ABC	Artificial Bee Colony
SDA	Spiral Dynamic Algorithm
EMA	Electromechanical Actuator
PLC	Programmable Logic Controller
A/D	Analog To Digital
D/A	Digital To Analog
CPU	Central Processing Unit

Pre-Proof Copy

2.0 METHODS AND MATERIALS

2.1 Construction of electromechanical servo system

In robot control, the setting of the electromechanical axis can meet the general structure and joint control of the robot. However, further research is currently being done on how to improve the accuracy of robots. In general, the number of slots in the motor in mechatronics is the key to motor control, and its data parameters will affect the control accuracy and cost of the motor. According to the analysis of the changes in the winding of the electric slot, the size of the number of slots in the electric slot is shown in equation (1) [13].

$$w = \frac{Z}{2xp} \quad (1)$$

In equation (1), w represents the proportion of slots in the motor, Z represents the number of slots in the stator of the motor, x represents the number of phases in the motor, and p represents the logarithm of the number of poles in the motor slots. Parameters such as the number of motor windings and coil diameter are selected by considering motor control accuracy and cost. In practice, these parameters are typically subjected to a theoretical analysis, the objective of which is to ascertain the approximate range of parameters based on the operating principle and control requirements of the motor. Furthermore, the effect of different parameters on motor performance is predicted through the simulation analysis of the motor system. Finally, the parameters are optimized and adjusted according to the results of simulation and experimentation. When the proportion of battery stages is less than 1, the number of winding coils in the electrode slot can effectively increase the full slot rate of the battery, reduce the harmonic electromotive force of electric shock, and improve the balance of motor torque. The energy consumption of the entire motor is reduced. Therefore, to ensure the safety of the motor, the number of winding wires of the motor is increased, and parameter analysis is carried out for different turns and heating conditions, as shown in equation (2) [14].

$$m = \frac{4S}{\pi a D^2}\eta \quad (2)$$

In equation (2), m represents the number of motor coil windings, S represents the stator slot area of the motor (mm2), D represents the diameter of the motor coil winding group (mm), a represents the number of parallel coils of the motor coil winding, and η represents the proportion of the motor slot winding group to the slot area. There is a limit to the current passing through the coil of the battery cell, and the judgment criteria are selected based on the mesh size of the current and the diameter of the coil. The judgment expression is shown in equation (3) [15].

$$J = \frac{4I}{\pi a d^2} \quad (3)$$

In equation (3), J represents the current density passing through (A/mm2) and I represents the current passing through the coil winding (A). According to the parameter requirements of different motors, different motor structures and parameters need to be set, and different structures need to be optimized and analyzed. The motor shaft is designed with a hollow structure, and the controller and encoder are built into the shaft and connected to external devices through coils. At the same time, the motor system adopts a structure of multi-stage coil magnetic rings connected, and the two magnetic rings are fixed by stacking. The different components of the motor's casing and bottom are connected to form a whole, and it is isolated from the external environment through the casing. Finally, an encoder and decoder for controlling motor parameters are installed on the motor casing, and the motor is sealed with silicone. To determine the parameters of the motor and the system control requirements, the main control system of the motor is designed and constructed [16]. The structure of the motor control system is shown in Figure 1.

Pre-Proof Copy

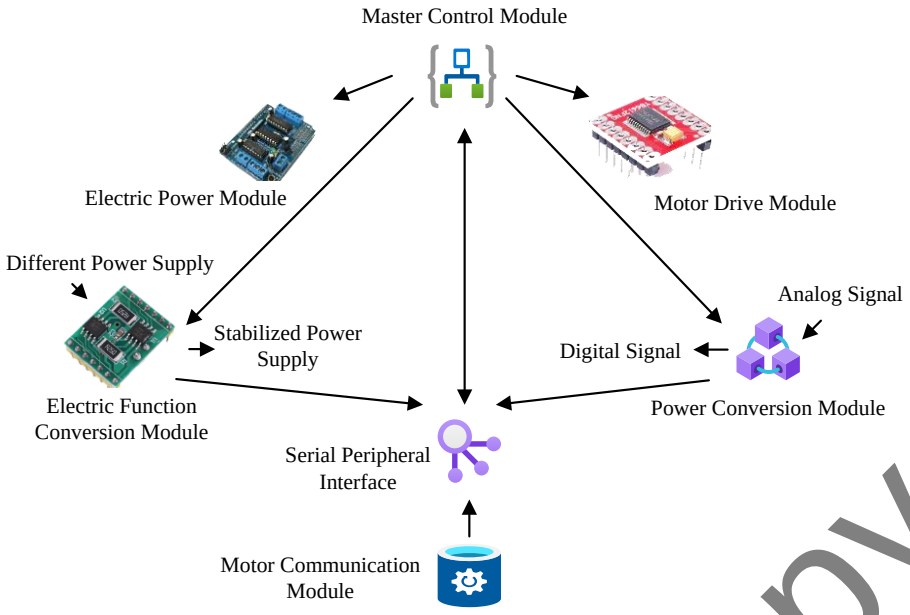

Figure 1. Structure of motor control system

From Figure 1, the control modules in the motor control system include the motor energy conversion module, main control module, power conversion module, motor drive module, electric power module, and motor communication module. The motor energy conversion module is responsible for converting the various power inputs into a stable power supply for the motor control system. This module includes power adapters, voltage regulators, and filters to ensure a stable and clean power supply. The main control module acts as the heart of the system and contains a microcontroller or microprocessor for executing algorithms and processing input signals from sensors. This module is responsible for coordinating the operation of the entire system, including motor start, stop, speed, and direction control. The power conversion module is capable of converting the digital signals from the main control module into the analog signals required to drive the motor. It includes drive circuits, power amplifiers, and protection circuits. The motor drive module is capable of directly controlling the operation of the motor and includes an H-bridge circuit or similar power electronics to regulate the motor's current and voltage. The power module is capable of managing the distribution of power to the motor control system, ensuring that all components receive the proper voltage and current. The module includes power distribution units, relays, and fuses. The motor communication module is responsible for exchanging data with other systems or modules. Modules include serial communication interfaces, network interfaces, or other communication protocols. In the hardware circuit of the entire motor, different components have different supply voltages and changes in voltage can affect the normal operation of circuit components. Therefore, most circuit components must ensure stable and appropriate voltage levels. The voltage supply legend for motor conversion is shown in Figure 2.

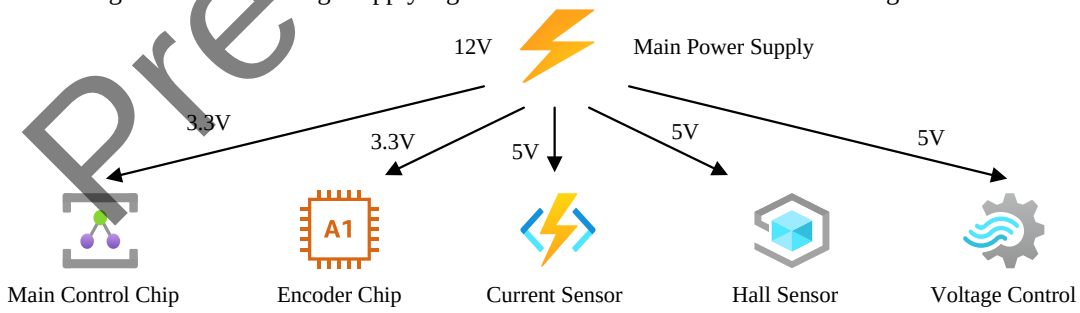

Figure 2. Legend of voltage supply for motor conversion

From Figure 2, during the voltage configuration, the main power supply can provide a voltage intensity of 12V and deliver voltage to different parts. The voltage of the main control chip is controlled at 3.3V, the chip size of the encoder is controlled at 3.3V, the voltage of the current sensor and Hall sensor is controlled at 5V, and the voltage of the entire circuit is controlled at 5V.

2.2 Optimization of the electromechanical servo system

Considering the actual working environment and the control accuracy of electromechanical systems, this study investigates the use of DMCA for control analysis of electromechanical servo systems to improve their control accuracy. The system requires a large torque in general working environments, so the DMCA is used to drive and optimize the

Pre-Proof Copy

control process of the electromechanical servo system. The permanent magnet electromechanical system has multiple system control methods, such as vector control and torque control. Accurate control of electromechanical output current, output torque, and position can be achieved through vector control of electromechanical systems. In the process of electromechanical control, current is the foundation of the entire electromechanical control. Controlling the current of the electromechanical servo system will greatly improve the accuracy of the entire system. The process of the electromechanical control program is shown in Figure 3.

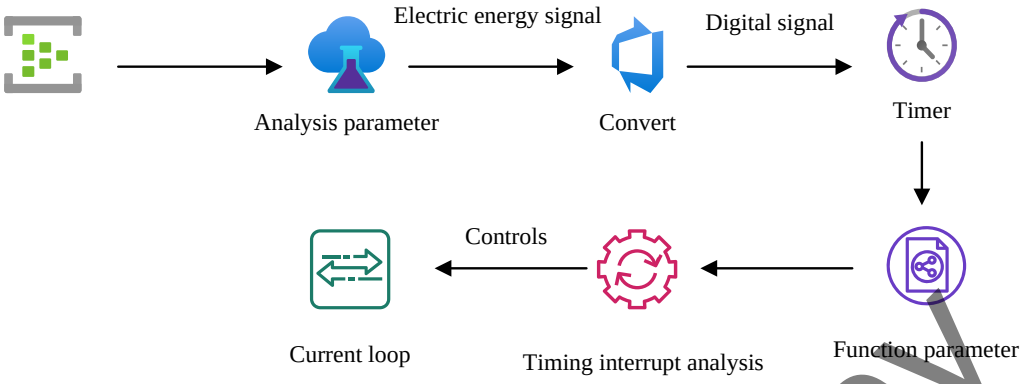

Figure 3. Mechanical and electrical control program process

From Figure 3, in the process of electromechanical control, the program will first perform data initialization configuration and then initialize and analyze the parameters of the electromechanical system. By simulating the digital conversion in electromechanical systems, the electrical energy signal will be converted into a digital signal for processing and analyzing data from analog sensors. Secondly, by using a timer, it is possible to perform timed interrupt analysis on the function parameters in the electromechanical system and finally complete the control of the current loop. To ensure the overall control of the motor, a timer is used in the interrupt program to control the speed and current commands of the motor. The interruption control process of the electromechanical servo system is shown in Figure 4.

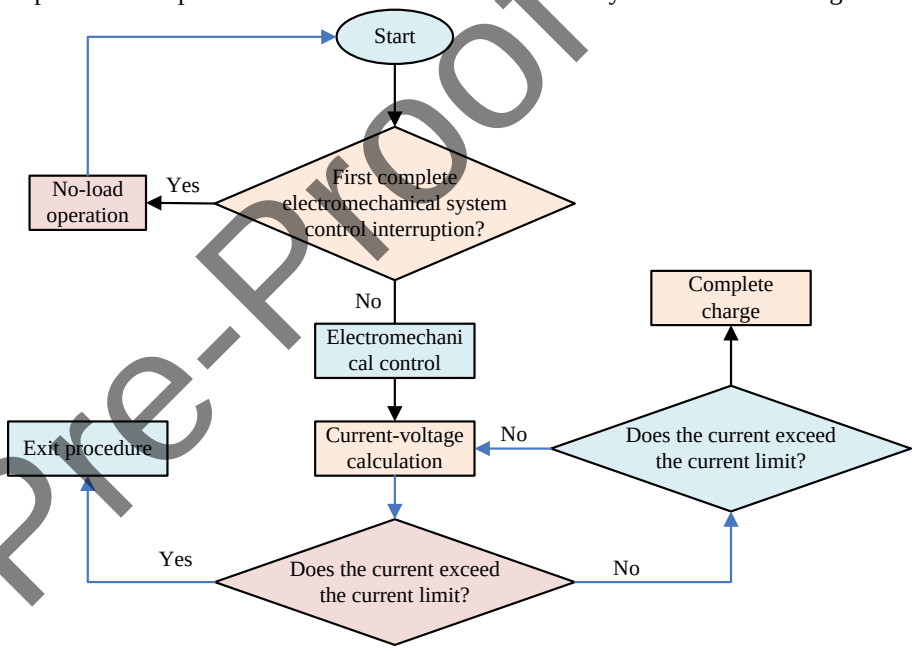

Figure 4. Interrupt control process of electromechanical servo system

From Figure 4, in the interrupt control of the electromechanical servo system, it is necessary to determine whether the control interrupt of the electromechanical system is completed for the first time. If not, the system will operate without load. If not, the system will perform electromechanical control, calculate current and voltage through three-phase current devices, and then determine whether the current will exceed the current limit. If there is, it will exit the program. If not, the charging status of the electromechanical servo system will be judged to determine whether the charging is completed. If it is completed, the interruption will be completed by controlling parameters such as system speed and current. If not possible, it will recalculate the electrical angle, speed, and position and then determine if the charging is complete. The electromechanical servo system obtains the magnitude of the electromechanical angle value through angle compensation, as shown in equation (4).

$$\theta_m^s(x) = \theta_m(x-2) \quad (4)$$

Pre-Proof Copy

In equation (4), $\theta_m^s(x)$ represents the mechanical angle in the electromechanical servo system at time x and $\theta_m(x-2)$ represents the actual mechanical motion angle of the servo system at time $x-2$. The actual motor angle value is shown in equation (5) [17].

$$\theta_e^s(x) = p * \theta_m^s(k) = p * \theta_m(k-2) \quad (5)$$

In equation (5), $\theta_e^s(x)$ represents the actual motor angle value of the electromechanical servo system at time x, and p represents the number of electrode pairs. The system angle at the next moment is shown in equation (6) [18].

$$\theta_e^s(x) = p * \theta_m^s(x-1) = p * \theta_m(x-3) \quad (6)$$

In equation (6), $\theta_m^s(x-1)$ represents the mechanical angle value at time $x-1$, and $\theta_m(x-3)$ represents the mechanical angle value at time $\theta_m(x-3)$. The magnitude of the change in motor angular velocity at the next moment is shown in equation (7).

$$w_e(x) = (\theta_e^s(x) - \theta_e^s(x-1))/T \quad (7)$$

In equation (7), $w_e(x)$ represents the electromechanical angular velocity at time x, and T represents the current cycle of the electromechanical system. The actual motor angle size obtained from the final motor is shown in equation (8) [19].

$$\theta_e(x) = \theta_e^s(x) + w_e(x) * 2T = p * \theta_m(x-2) + w_e(x) * 2T \quad (8)$$

After controlling the current command of the electromechanical system through the servo system, the virtual system voltage AC value voltage is obtained, and then the three-phase voltage is obtained by voltage transformation. At the same time, to improve the control accuracy of the three-phase motor and servo system, the mechanical angle size is calculated and transformed as shown in equation (9) [20].

$$\theta_e(x+1.5) = \theta_e^s(x) + w_e(x) * 3.5T = p * \theta_m(x-2) + w_e(x) * 3.5T \quad (9)$$

In equation (9), $\theta_e(x+1.5)$ represents the actual electromechanical angle magnitude at time $x+1.5$. The optimization control of voltage in the electromechanical servo system requires adjusting the height of the pulse voltage and calculating the duty cycle, as shown in equation (10) [21-22].

$$D_{PWM} = \frac{PDC}{PTPER} * 100\% \quad (10)$$

In equation (10), D_{PWM} represents the pulse duty cycle of the servo system, PDC represents the voltage height count of the pulse, and $PTPER$ represents the total number of pulses. The voltage magnitude is calculated through current transformation to obtain the voltage height count of the pulse. Then, the power supply to the busbar is directly completed through a three-phase voltage circuit. In the speed control of the electromechanical servo system, the speed control requires a PID control system, as shown in Figure 5, for the speed control process of the motor.

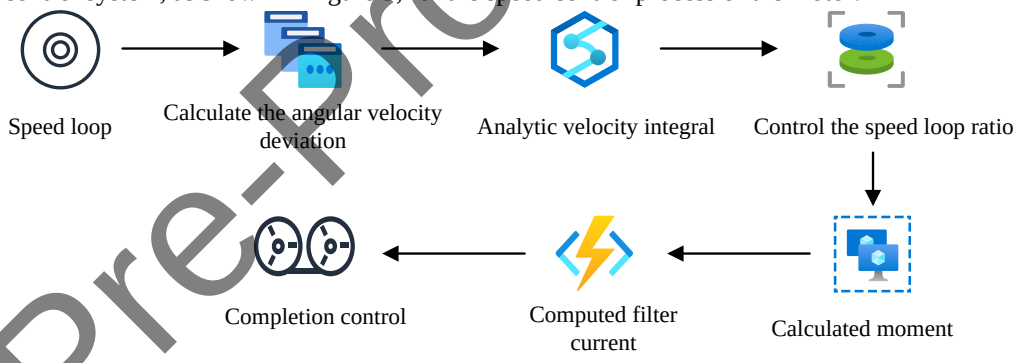

Figure 5. Motor speed control process

From Figure 5, in the control of the servo system, the manipulation of the electromechanical speed requires the use of speed commands to indicate the analysis of the deviation angular velocity offset value of the electromechanical system. Then, the integration of speed is used to calculate the velocity integration and angular velocity offset. Next, proportional control of the speed loop is performed, the system's torque, filtering current, etc., are calculated, and finally, the control of the speed loop is completed. Therefore, to improve the speed control and precision of the electromechanical system, the mechanical angle of the servo system is optimized, and 32-bit and 2 * 32 pulses are used for setting and encoding the electromagnetic encoder. The analysis of joint stiffness control in electromechanical servo systems is an important means to enhance system control. An algorithmic dual-axis control scheme is used to control and drive the joints of electromechanical systems, i.e., using dual motors to drive the joints. Two motors are fixed on the joint, and when the joint is stationary, the motors will output torque in opposite directions together. During joint movement, the bidirectional motor provides forward torque, making the forward torque of the motor greater than the reverse torque. To ensure the collaborative control effect of the servo system, a communication design is carried out for the command signals of the main control motor during algorithm control. Different current loops and current conversion algorithms are used to transmit and control the communication signals of the electromechanical system. The process of the electromechanical control system is shown in Figure 6.

Pre-Proof Copy

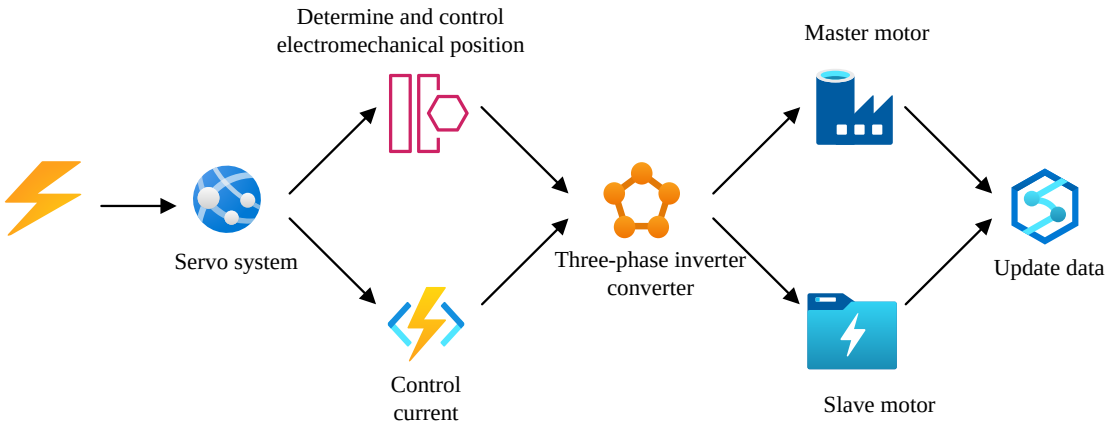

Figure 6. Mechanical and electrical control system process

From Figure 6, in the control of the algorithm's electromechanical servo system, when the servo system receives a current signal, it first judges and controls the position of the electromechanical system, then controls the speed of the electromechanical system through pulse signals and controls the current through current conversion. It converts the current signal through a three-phase inverter to control the main control motor. At the same time, the control of the control motor is also carried out through a three-phase inverter. Finally, the data parameters are fed back into the system to update the speed, position, and current. The conversion method between the main control motor and the slave control motor is shown in equation (11) [23-25].

$$\begin{cases} i_{qref1} = i_{qref} + I_e \\ i_{qref1} = I_c \end{cases} \quad (11)$$

In equation (11), i_{qref1} represents the current signal from the master control to the slave control motor, i_{qref} represents the outgoing signal current of the master control motor, and I_c represents the stable specified current. When the value of i_{qref} is greater than or equal to 0, the current signal output of the main control motor is $i_{qref1} = i_{qref} + I_e$. When the value of i_{qref} is less than 0, the current signal output of the main control motor is $i_{qref1} = I_c$. The motor current is controlled as shown in equation (12) [26-27].

$$\begin{cases} i_{qref2} = I_e \\ i_{qref2} = I_c - i_{qref} \end{cases} \quad (12)$$

In equation (2), i_{qref2} represents the current signal from the master control to the slave control motor. When the value of i_{qref} is greater than or equal to 0, the current signal output of the main control motor is $i_{qref2} = I_e$. When the value of i_{qref} is less than 0, the current signal output of the main control motor is $i_{qref2} = I_c - i_{qref}$. When the DMCA is used for collaborative control, the quality control motor needs to send motor command signals to the slave motor. However, due to interference during signal transmission outside the motor, STM32H750 is used as the communication motherboard for external communication optimization of the electromechanical servo system, and the Serial Peripheral Interface (SPI) communication mode is used. The motherboard driver uses AM26C31QDR position motherboard driver main components, and the differential signal board uses STM32 for power transmission signals. The final optimized electromechanical servo system includes main components such as master control, slave control, controller, communication board, etc [28-29].

3.0 RESULTS AND DISCUSSION

To verify the practical application effect of the optimized electromechanical servo system, the parameter settings of the electromechanical servo system have been studied. The control cycle of the electromechanical system has been set to 45.0 us, the back electromotive force coefficient has been set to 0.170V/(rad/s), the torque coefficient has been set to 0.162 N*M/A, the power supply was switch power supply, the current loop d-axis proportional coefficient was 1050.0, and the d-axis integral coefficient was 1550.0. The current loop had a q-axis proportional coefficient of 980.0 and a q-axis integral coefficient of 1520.0. The d-axis inductance size was 0.002 H, and the q-axis inductance size was 0.0015 H. The system had a moment of inertia of 0.00085 kg*m^2 and a power supply voltage of 15V. It has set a cyclic operation command for the system, set the maximum rotational speed of the electromechanical system to 31.42 rad/s, and set the acceleration and deceleration time of the electromechanical system to 0.03 seconds. The theoretical rotation angle of the motor has been 68°.

Pre-Proof Copy

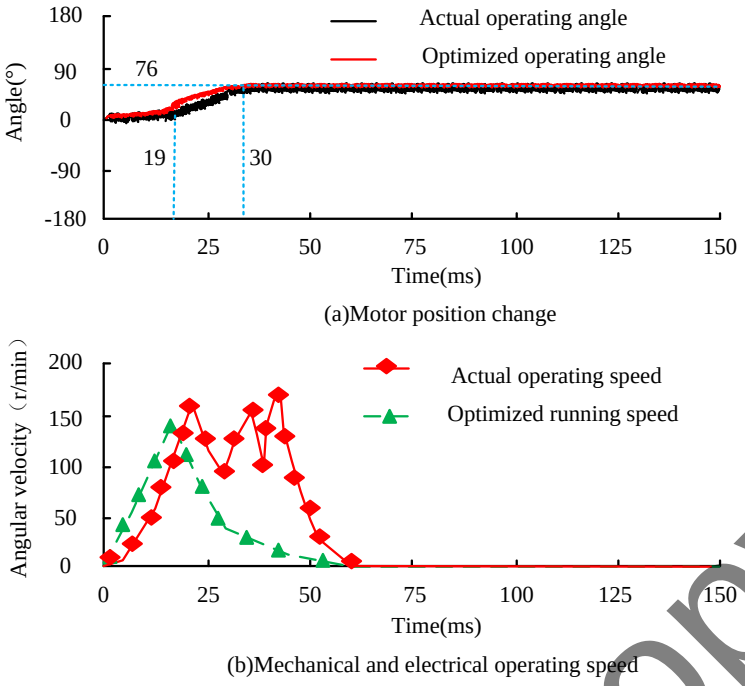

(a)Motor position change

(b)Mechanical and electrical operating speed

Figure 7. Changes in position and speed before and after system optimization

From Figure 7 (a), the position deviation angle of the electromechanical system varied between 19 ms and 30 ms when using the optimized electromechanical system. When a change occurred, it was the result of issuing a position command. From the comparison of the electromechanical system before and after optimization, the angle change of the optimized electromechanical system has been smoother compared to before optimization. The angle change of the electromechanical servo system had better performance improvement compared to before optimization, and the completion time of rotation was shorter. This may be the result of the system using collaborative control. From Figure 7 (b), after the system issued a rotation command, the unoptimized system exhibited fluctuations in angular velocity, with a total variation time of 0-60ms and a maximum variation angular velocity of 160 r/min. The optimized system showed a more obvious triangular command change in angular velocity, with a change time of 0-50ms and a maximum change in angular velocity of 145 r/min. It can be seen that the optimized system has significant improvements in both position movement and angle rotation. The comparison test of the changes in the electromechanical system under different instructions is shown in Figure 8.

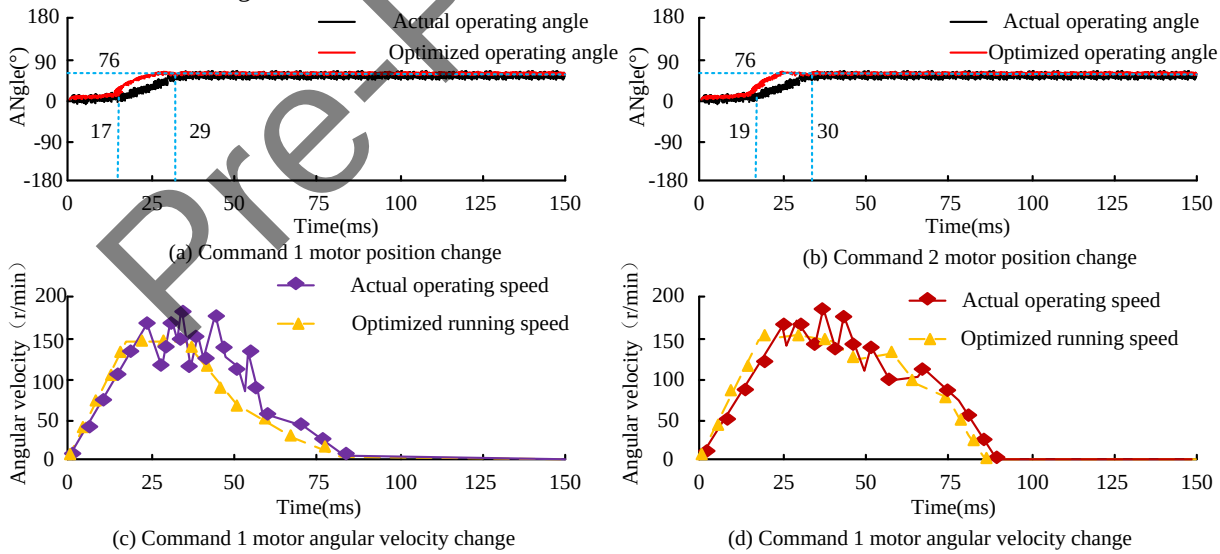

(a) Command 1 motor position change

(b) Command 2 motor position change

(c) Command 1 motor angular velocity change

(d) Command 1 motor angular velocity change

Figure 8. Changes in mechanical and electrical servo system parameters under different instructions

From the comparison between Figure 8 (a) and (b), the actual position and angle changes of the electromechanical system were not significantly different after issuing different commands and were basically at the same angle. However, there have been differences in the electromechanical change time at the same angle. The system angle change time under instruction 1 and instruction 2 has been between 17 ms and 29 ms. From the angle change curves of the two instructions, there have been good change curves in the system's instructions after the instruction was issued, with a faster change

Pre-Proof Copy

speed and higher change efficiency. From Figure 8 (c) and Figure 8 (d), the actual change curve of the system showed significant fluctuations after the instruction was issued, while the optimized curve showed regular upward and downward changes. The system optimized through algorithms had significant advantages in processing electromechanical control instructions. The processing effect of the system on instruction signals also showed good changes. The comparison and analysis of the angle changes of the system motor before and after optimization under different instructions are shown in Table 2.

Table 2. Changes in mechanical and electrical system angles under different instructions

/	Initial Angle(°)	Static angle 1 (°)	Static angle 2 (°)	Optimized stationary angle 1 (°)	Optimized stationary angle 2 (°)	End angle (°)
Command 1	0	46	72	52	76	0
Command 2	0	45	70	51	75	0
Command 3	0	46	68	55	80	0
Command 4	0	46	71	53	76	0
Command 5	0	45	69	52	78	0

From Table 2, under different instructions, the initial and final angles of the angle change of the electromechanical servo system have been both 0°. In actual electromechanical angle changes, the range of angle changes for electromechanical static angle 1 after issuing different commands has been between 45° and 46°, and the range of angle changes for static angle 2 has been between 68° and 72°. The angle changes of the system have been significantly improved under different optimized instructions, with the angle change being the most significant at 12°. This indicated that there was a good change and optimization effect in the system angle after algorithm optimization. The larger the angle change, the greater the amplitude of motion of the electromechanical system after receiving instructions, and the more obvious the effect of receiving instructions. The comparison of the motor rotation effects under multiple different instructions is shown in Figure 9.

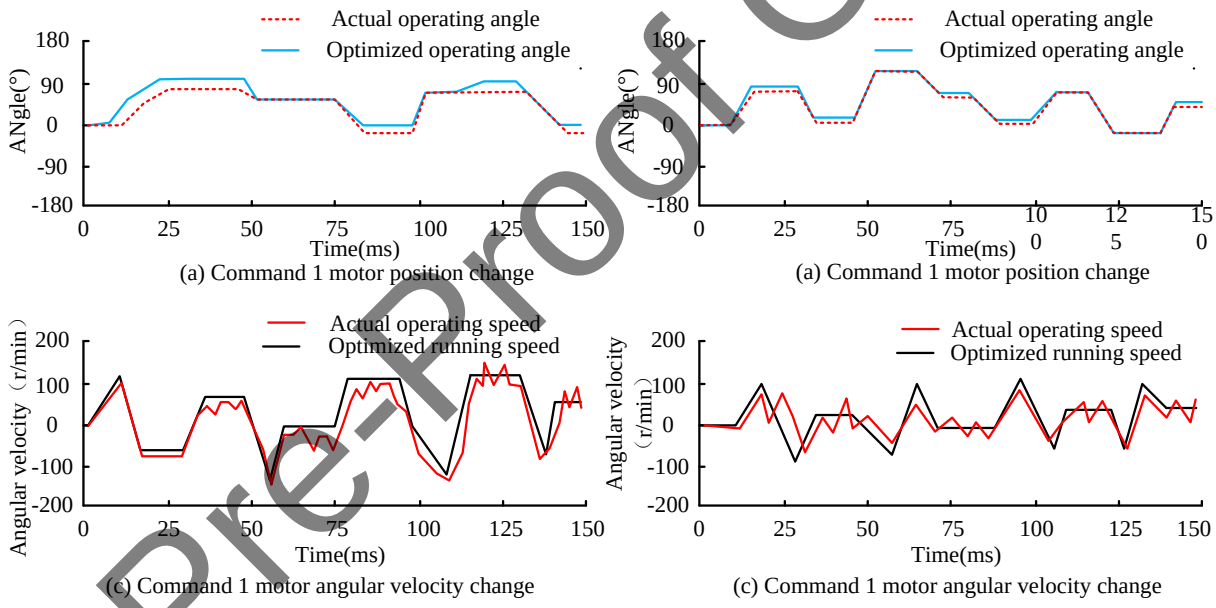

Figure 9. Comparison of motor rotation changes

From Figures 9 (a) and (b), in the comparison of different motor commands, the motor variation angle under the two commands has significantly improved after optimization, and the rotation angle also has significantly improved compared to before optimization. Among them, the angle with the largest change was 10 ° in Figure 9 (a). From Figure 9 (c) and Figure 9 (d), after receiving multiple commands, the optimized motor system has had a smoother change in angular velocity rotation, while the unoptimized motor showed fluctuating changes in angular velocity. In Figure 9 (c), the fluctuation amplitude of the motor has been larger between 120r/min and 130r/min. In Figure 9 (d), the angular velocity of the motor has varied significantly between 30r/min and 50r/min. This may be due to the poor conversion of current signals by unoptimized systems after receiving instructions. The comparative analysis of the optimized position changes of the motor is shown in Figure 10.

Pre-Proof Copy

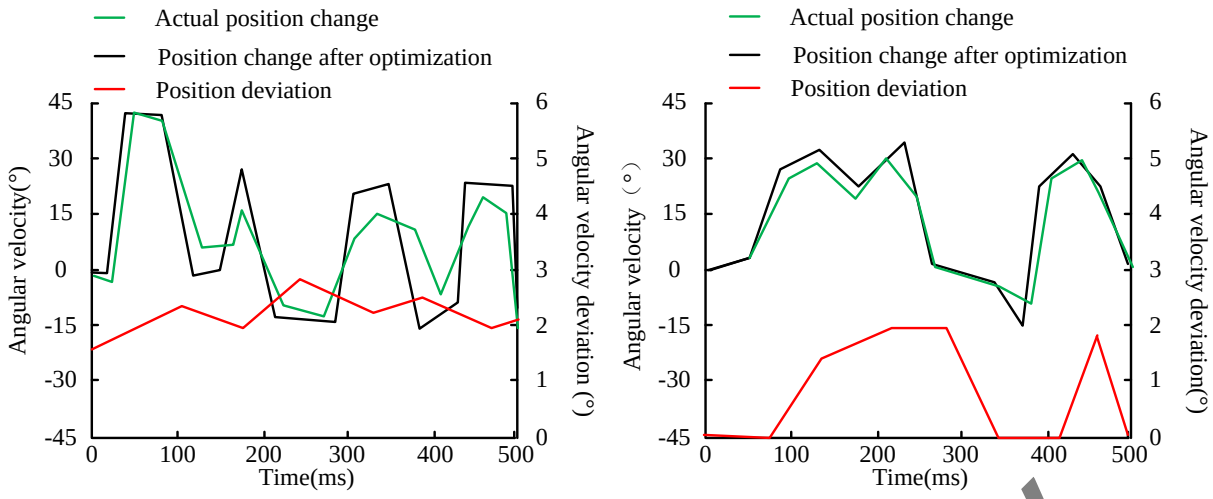

(a) Command 1 position change (b) Command 2 position change

Figure 10. Changes in system position deviation under different instructions

From Figure 10 (a), the position deviation range of the motor before and after optimization have been between 1° and 2°. This indicated that there have been a significant improvement in the system position change after algorithm control optimization, with a larger range of mechanical and electrical changes and a more obvious response process. From Figure 10 (b), the maximum variation in the position deviation of the electromechanical system could reach 2° after optimization, indicating that algorithm control optimization could effectively improve the electromechanical control effect of the system. To analyze the system deviation before and after optimization, the accuracy changes of the system were compared and shown in Table 3.

Table 3. Comparison of system accuracy changes

/	Command 1	Command 2	Command 3	Command 4	Command 5
Positioning accuracy 1 (°)	1.0	1.5	1.2	1.4	1.1
Positioning accuracy2 (°)	2.1	1.6	2.0	1.9	1.8
Positioning accuracy3 (°)	3.4	2.6	2.4	3.0	2.8
Positioning accuracy 4 (°)	2.4	2.5	2.4	2.2	2.3
Setting time 1(ms)	50.00	51.54	49.58	48.68	50.25
Setting time 2(ms)	53.68	53.84	54.85	56.67	58.95
Setting time 3(ms)	61.28	62.38	64.58	63.25	63.18
Setting time 4(ms)	66.29	68.96	70.24	69.84	71.25

The integration time in Table 3 represents the time required for the output of the motor to change from the initial state to the steady-state value and remain within a tolerance range of the steady-state value after receiving a step input. From the comparison of the position changes of different commands, the position change deviation of the motor at position change point 1 has been within 1.5°, indicating that the control amplitude change of the motor at this point was small and the optimization effect of the motor was not significant. The position change of the motor at point 3 was most significant in the optimization change of the motor, with the maximum change amplitude at 3.4°. The accuracy of the position change of the motor changed significantly after optimization, which also indicated that the control amplitude of the motor was more obvious after optimization. From the comparison of the integration time of the motors, the longest integration time at point 4 could reach 71.25ms, indicating that the motor at this point took a longer time to enter the steady state. This also suggested that the stability of the motor at this point was poor. However, from the perspective of the change position, the change control at this point was relatively stable, which also indicated that the motor control effect was significantly improved after algorithm optimization. To test the changes in the control parameters of the system using the algorithm optimization and not using the algorithm optimization under multiple tests, the speed feedback coefficient, position feedback coefficient, sampling time and control period of the system were compared and analyzed to obtain the results as shown in Table 4.

Table 4 Comparison of system control parameters before and after optimization

/	Algorithm optimization				No algorithm optimization			
Control parameter	Velocity feedback gain(V/(m/s))	Position feedback gain(V/m)	Sampling time(s)	Control cycle time(s)	Velocity feedback gain(V/(m/s))	Position feedback gain(V/m)	Sampling time(s)	Control cycle time(s)

Pre-Proof Copy

1	2.35	54.52	3.52	2.65	1.25	36.42	5.38	4.85
2	2.34	56.35	3.52	2.87	1.35	36.84	5.26	4.75
3	2.35	55.15	3.44	2.48	1.22	36.48	5.14	4.36
4	2.68	54.84	3.02	2.68	1.68	35.15	5.36	4.65
5	2.22	54.89	3.15	2.55	1.24	36.20	5.13	4.55

From Table 4, the control parameters of the system using algorithmic optimization and without algorithmic optimization have been in a more stable range for different numbers of tests. However, the values of the system parameters were better for all the systems controlled using algorithmic optimization. Among them, the larger the speed limitation and position limitation coefficients indicated that the system was better, in which the position limitation of the system optimized with the algorithm could reach a maximum of 56.35V/m, and the speed limitation could reach a maximum of 2.68V/(m/s). It can be seen that the control system of the system optimized with the algorithm has been in a better value, and the system accuracy has been higher and more stable. At the same time, the smaller the sampling time and control period of the system, the more stable the system was, and the sampling time and control period of the current system optimized with the algorithm had lower control parameters compared to the system not optimized with the algorithm. This shows that the algorithm can effectively improve the control parameters of the system.

4.0 CONCLUSION

This study aimed to address the issues of poor motor control performance and insufficient encoder reading accuracy in current research, as well as optimize and improve the encoder structure and circuit board control of the electromechanical servo system. The DMCA was used to optimize and improve the motor servo system. The research results indicated that the optimized electromechanical position deflection angle varied between 19 ms and 30 ms, and the optimized system took less time to complete rotation, resulting in a more significant control effect. The maximum rotational angular velocity of the system was 160 r/min. The maximum rotational angular velocity was 145 r/min when the change time was between 0-50 ms. In the changes of different command electromechanical systems, the system change curve after issuing the command was smoother and more stable, and the change efficiency was higher. In the static electromechanical angle change of instruction 1, the angle change was between 45°-46°, and the angle change at point 2 was between 68°-72°. The maximum angle change after optimization was 12°. The maximum angle change of the optimized electromechanical servo system under multiple commands was 10°, and the maximum angular velocity change was between 120 r/min and 130 r/min. The position change angle range of the optimized system was 1°-2°. The position deviation after system optimization was within 1.5°, with the maximum position change at point 3 being 3.4° and the longest integration time at point 4 being 71.25 ms. It can be seen that optimizing the system through algorithm control can effectively improve the control accuracy and effectiveness of the electromechanical servo system. Although some achievements have been made in the research, there are still some shortcomings in the current research. For example, the study only optimized the encoder and system of the servo system and analyzed it only through a single position change parameter. Therefore, in future research, precise control of the system will be studied through different parameters. The optimized motor control system in current research has improved control accuracy and dynamic response, but there are limitations in scalability. Therefore, in future research, DMCA will be compared with other emerging control algorithms, especially in specific applications such as robotics and aerospace systems. Although DMCA improves system performance, its cost-effectiveness ratio is not yet clear. Therefore, in future research, the possibility of combining DMCA with intelligent control strategies will be explored to enhance the system's adaptability and robustness in complex and uncertain environments.

ACKNOWLEDGEMENTS
The author/s would like to acknowledge …….

CONFLICT OF INTEREST
The authors declare that they do not have any conflict of interest.

AUTHORS CONTRIBUTION
Wei Lu conducted experiments, recorded data, analyzed the results，and wrote a manuscript. Wei Lu agreed to the published version of the manuscript.

5.0 REFERENCES

[1] S. Autsou, K. Kudelina, T. Vaimann, A. Rassõlkin, and A. Kallaste, "Principles and methods of servomotor control: Comparative analysis and applications," *Applied Sciences*, vol. 14, no. 6, pp. 2579-2581, 2024.

[2] Y. Long, J. Du, K. Yang, and S. Yuan, "Modelling of a direct-driven electromechanical actuation system based on the Lagrange-Maxwell equation," *IET Electric Power Applications*, vol. 15, no. 11, pp. 1438-1451, 2021.

Pre-Proof Copy

[3] J. Huang, Z. Song, S. Li, and J. Ruan, "Claw-pole magnetic levitation torque motor for 2D valve with automatic neutral adjustment," *IET Electric Power Applications*, vol. 17, no. 10, pp. 1285-1303, 2023.

[4] H. Jin, X. Zhao, and T. Wang, "Adaptive backstepping complementary sliding mode control with parameter estimation and dead-zone modification for PMLSM servo system," *IET Power Electronics*, vol. 14, no. 4, pp. 785-796, 2021.

[5] S. Thangavel, C. Maheswari, and E. B. Priyanka, "Dynamic modeling and control analysis of industrial electromechanical servo positioning system using machine learning technique," *Journal of Testing and Evaluation*, vol. 49, no. 4, pp. 2425-2440, 2021.

[6] A. Aimasso, P. C. Berri, and M. D. L.Dalla Vedova, "A genetic-based prognostic method for aerospace electromechanical actuators," *International Journal of Mechanics and Control*, vol. 22, no. 2, pp. 195-206, 2021.

[7] H. Zhang, J. Y. Zhao, Y. F. Wang, Z. H. Zhang, H. G. Ding, and J. X. Man, "Electro-hydraulic position servo system based on sliding mode active disturbance rejection compound control," *Proceedings of the Institution of Mechanical Engineers, Part C: Journal of Mechanical Engineering Science*, vol. 236, no. 5, pp. 2089-2098, 2022.

[8] X. Chen, W. Deng, J. Yao, X. Liang, and Z. Zhang, "Robust indirect adaptive control of electromechanical servo systems with uncertain time-varying parameters," *International Journal of Control*, vol. 96, no. 4, pp. 870-883, 2023.

[9] H. Hu, Q. Zhang, J. Fang, T. Wang, and J. Wei, "Practical adaptive robust tracking control of the dual-valve parallel electro-hydraulic servo system with reduced-order model," *Transactions of the Institute of Measurement and Control*, vol. 46, no. 3, pp. 501-512, 2024.

[10] M. S. Hossain, I. Sultan, T. Phung, and A. Kumar, "A Literature Review of the Design, Modeling, Optimization, and Control of Electro-Mechanical Inlet Valves for Gas Expanders," *Energies*, vol. 17, no. 18, pp. 4569-4570, 2024.

[11] L. Zhang, C. Zhang, P. Wang, M. Shabaz, S. M. G., and K. H. Kishore, "Realization of optimization design of electromechanical integration PLC program system based on 3D model," *Nonlinear Engineering*, vol. 12, no. 1, p. 20220252-20220253, 2023.

[12] A. A. Hashim, N. M. Ghani, S. Ahmad, and A. N. Nasir, "System Identification and Control of Linear Electromechanical Actuator Using PI Controller Based Metaheuristic Approach," *Applications of Modelling and Simulation*, vol. 8, no. 3, pp. 213-224, 2024.

[13] G. Sun, J. Zhao, and Q. Chen, "Observer-based compensation control of servo systems with backlash," *Asian Journal of Control*, vol. 23, no. 1, pp. 499-512, 2021.

[14] G. Yang, T. Zhu, F. Yang, L. Cui, and H. L. Wang, "Output feedback adaptive RISE control for uncertain nonlinear systems," *Asian Journal of Control*, vol. 25, no. 1, pp. 433-442, 2023.

[15] X. Yang, A. Shi, J. Xuan, and Z. Yang, "Analytical prediction and analysis of the detent force with the feedback harmonics for the direct drive motion system," *IET Power Electronics*, vol. 16, no. 13, pp. 2192-2202, 2023.

[16] G. Yang and J. Yao, "Multilayer neurocontrol of high-order uncertain nonlinear systems with active disturbance rejection," *International Journal of Robust and Nonlinear Control*, vol. 34, no. 4, pp. 2972-2987, 2024.

[17] B. Bai, Z. Li, J. Y. Zhang, D. Q. Zhang, and C. W. Fei, "Research on multiple-state industrial robot system with epistemic uncertainty reliability allocation method," *Quality and Reliability Engineering International*, vol. 37, no. 2, pp. 632-647, 2021.

[18] N. Nahak, O. Satapathy, and P. Sengupta, "A new optimal static synchronous series compensator-governor control action for small signal stability enhancement of random renewable penetrated hydro-dominated power system," *Optimal Control Applications and Methods*, vol. 43, no. 3, pp. 593-617, 2022.

[19] H. Shi, R. Li, X. Bai, Y. Zhang, L. Min, D. Wang, and Y. Lei, "A review for control theory and condition monitoring on construction robots," *Journal of Field Robotics*, vol. 40, no. 4, pp. 934-954, 2023.

[20] D. Yang, X. Hai, Y. Ren, J. Cui, K. Li, and S. Zeng, "A hybrid fault prediction method for control systems based on extended state observer and hidden Markov model," *Asian Journal of Control*, vol. 25, no. 1, pp. 418-432, 2023.

[21] J. E. Naranjo, A. Valle, A. Cruz, M. Martín, M. Anguera, P. García, and F. Jiménez, "Automation of haulers for debris removal in tunnel construction," *Computer-Aided Civil and Infrastructure Engineering*, vol. 38, no. 14, pp. 2030-2045, 2023.

[22] H. Qiang, M. A. Ikbal, and S. Khanna, "Prediction of energy consumption of numerical control machine tools and analysis of key energy-saving technologies," *IET Collaborative Intelligent Manufacturing*, vol. 3, no. 3, pp. 215-223, 2021.

[23] H.Mokayed, T. Z.Quan, L.Alkhaled, and V.Sivakumar, "Real-time human detection and counting system using deep learning computer vision techniques," Artificial Intelligence and Applications,vol. 1, no. 4, pp. 221-229, 2023.

[24] X. Dong, Q. Fan, and D. Li, "Detrending moving-average cross-correlation based principal component analysis of air pollutant time series," *Chaos, Solitons & Fractals*, vol. 172, p. 113558, Jul. 1, 2023.

[25] K. Udaichi, R. Chinaveer Nagappan, M. Garcia-Torres, P. B. Divakarachari, and S. N. Bhukya, "Large-scale system identification using self-adaptive penguin search algorithm," *IET Control Theory & Applications*, vol. 17, no. 17, pp. 2292-2303, Nov. 2023.

[26] J. Shi, P. Zhang, H. Hou, W. Cao, and L. Zhou, "Optimization of servo accuracy of Y axis of dicing saw based on iterative learning control," *International Journal of System Assurance Engineering and Management*, pp. 1-3, Apr. 6, 2024.

[27] M. Liu, C. Li, Y. Lei, and P. Dai, "PID control parameter optimization of servo system based on particle swarm optimization," *Journal of Physics: Conference Series*, vol. 2460, no. 1, p. 012166-012167, 2023,

[28] X. Wang, B. Chen, J. Dhupia, J. Bronlund, J. Han, W. Xu. "Conceptualization and Mechanical Design of a Cam-Follower Based Chewing Robot with Three Oral Chambers." IEEE Access, vol. 5, no. 10, pp. 2169-3536, Feb. 5, 2025.

Pre-Proof Copy

[29] H. Hua, X. Wu, X. Chen, H. Kong, Y. Sun, Q. Yang, M. C. Tavares, P. Naidoo. "Carbon reduction oriented regional integrated energy system optimization via cloud-edge cooperative framework." *CSEE Journal of Power and Energy Systems*, vol. 10, no. 1, pp. 1-12, Jan. 10, 2025.

Pre-Proof Copy